

Microwave Plasma Synthesis of Nanostructured γ - Al_2O_3 Powders

L. Fu, D. Lynn Johnson,^{*,†} Jian G. Zheng, and Vinayak P. Dravid*

Department of Materials Science and Engineering, Northwestern University, Evanston, Illinois 60208-3108

Nanostructured Al_2O_3 powders have been synthesized by combustion of aluminum powder in a microwave oxygen plasma, and characterized by X-ray diffraction and electron microscopy. The main phase is γ - Al_2O_3 , with a small amount of δ - Al_2O_3 . The particles are truncated octahedral in shape, with mean particle sizes of 21–24 nm. The effect of reaction chamber pressure on the phase composition and the particle size was studied. The γ -alumina content increases and the mean particle size decreases with decreasing pressure. No α - Al_2O_3 appears in the final particles. Electron microscopy studies find that a particle may contain more than one phase.

I. Introduction

BECAUSE of fine particle size, high surface area, and high activity of the surfaces, the transition aluminas find wide applications in industry as adsorbents, catalysts or catalyst carriers, coatings, and soft abrasives. Thus, enormous efforts have been devoted to understanding the synthesis of nano-sized aluminas and the nature of the transformations and crystal structures of the various phases.^{1–5} Among the transition aluminas, γ - Al_2O_3 , usually produced from boehmite, is an extremely important technological material.^{6–8} The γ (and, to some extent, δ and θ) alumina is used as a catalyst support material in the automotive industry, a catalyst itself in petroleum refining, and an electrolytic oxide layer on aluminum.

In this communication, microwave plasma combustion synthesis of nanostructured γ - Al_2O_3 powders is reported.

II. Experimental Procedure

The system consisted of a 2.45 GHz microwave generator (Model GL 119, Gerling Laboratories, Modesto, CA) feeding a vertical single mode cylindrical cavity (Model MCR, Wavemat, Inc., Plymouth, MI). The reaction chamber was a 38 mm diameter quartz tube that passed coaxially through the center of the cavity. The pressure in the reaction chamber was controlled by throttling a downstream vacuum pump. An aluminum powder aerosol was generated and injected upward into the reaction chamber, where an upward flow of oxygen carried the powder into the plasma. The powder vaporized and reacted with oxygen to form the oxide, which was collected in a liquid nitrogen-cooled thermophoretic collector.

Aluminum powder (Alfa Aesar, Ward Hill, MA) was used as the precursor. The particle size was 7–15 μm with irregular shape.

The oxygen flow rate was 550 mL/min (STP). The microwave source power was 700 W. The pressure of the reaction chamber was set at 40, 80, and 100 torr to study the influence of plasma pressure on the phase composition and the particle size of the powder.

Phase analysis was conducted using X-ray diffractometry (OMAX-A, Rigaku, Tokyo, Japan) with nickel-filtered $\text{CuK}\alpha$ radiation at 40 kV and 20 mA. A 2θ range from 20° – 90° was covered at a scanning rate of $0.02^\circ/\text{min}$. The size, morphology, and crystal structure of the alumina powders were investigated by a field emission gun (FEG; Model HF-2000, Hitachi, Tokyo, Japan) and transmission electron microscope (TEM; Model H-8100; Hitachi, Japan). The particle-size distribution was determined by measuring more than 350 particles on the TEM images.

III. Results and Discussion

Figure 1 shows the XRD spectra of the powders prepared at pressures of 40, 80, and 100 torr. The main diffraction peaks correspond to γ - and δ -alumina, with γ -alumina predominating. Homogeneous nucleation at the high quenching rate results in the formation of these nonequilibrium phases instead of the stable α -alumina. The presence of the δ phase can be ascribed to transformation from the γ phase during cooling in the plasma tail gas. Because this cooling is rapid, only a small amount of γ phase is transformed to δ .

Figure 1 shows that γ -alumina decreases and δ increases slightly with increasing pressure in the reaction chamber. This is because the number of collisions within the plasma increases with increasing chamber pressure, causing the temperature of the heavy particles in the plasma (ions, atoms, and molecules) to increase as the pressure increases.⁹ Thus, both the temperature of the plasma flame as well as the temperature of the plasma tail gas is enhanced with increasing pressure, which results in relatively more γ -alumina transforming to δ .

The morphology of the particles synthesized at chamber pressures of 40, 80, and 100 torr is shown in Fig. 2. The particle shape

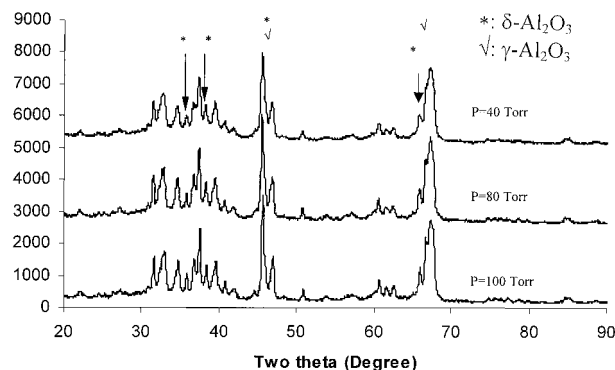


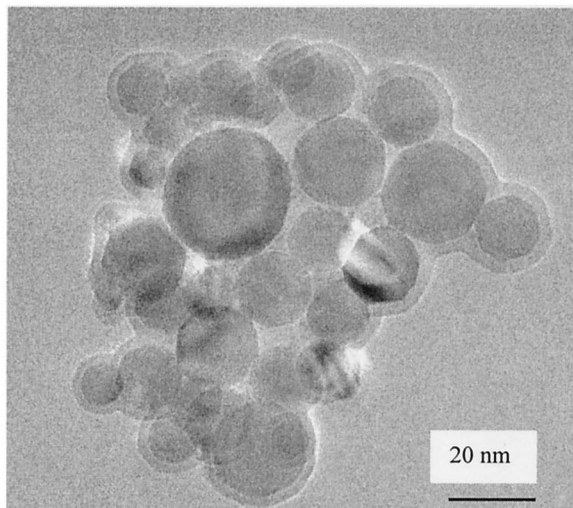
Fig. 1. XRD patterns of nanostructured alumina powders prepared at 40, 80, and 100 torr.

J.R. Groza—contributing editor

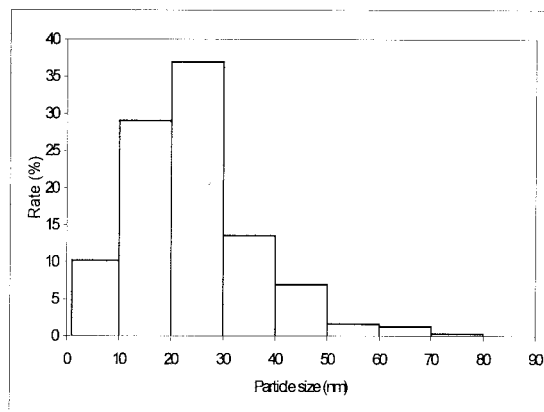
Manuscript No. 186917. Received June 27, 2002; approved March 15, 2003. Supported by the National Science Foundation through the Institute for Environmental Catalysis of Northwestern University, Grant No. CHE-9810378/004.

*Member, American Ceramic Society.

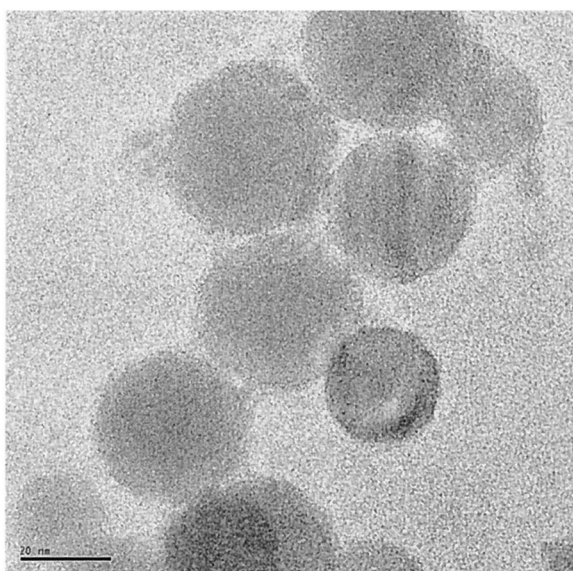
†Author to whom correspondence should be addressed. e-mail: dl-johnson@northwestern.edu.



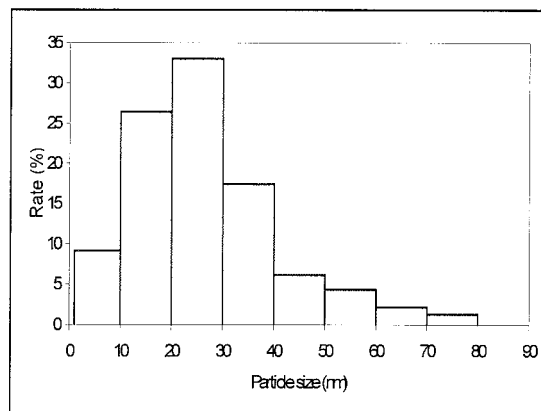
(a) 40 Torr



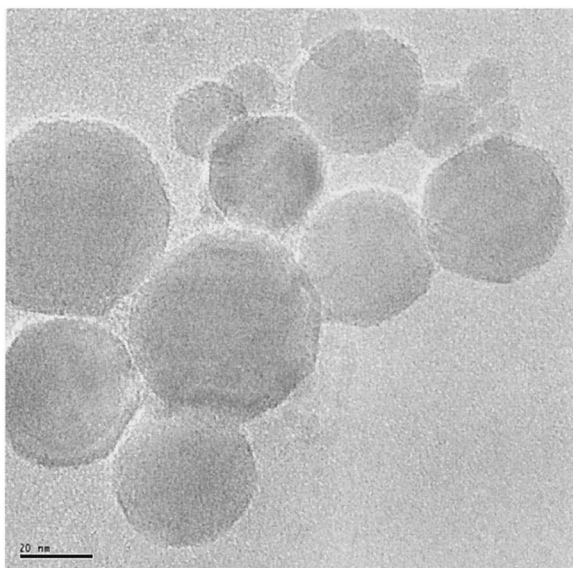
(a) 40 Torr



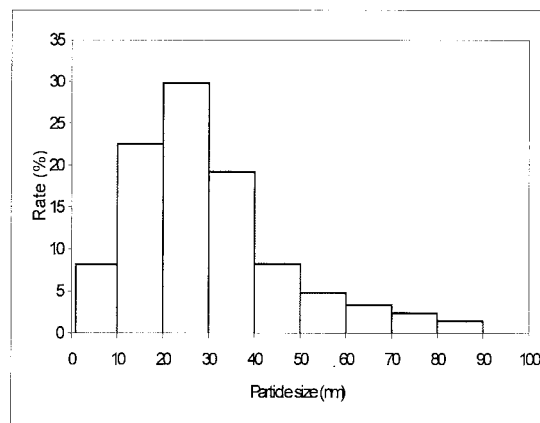
(b) 80 Torr



(b) 80 Torr



(c) 100 Torr



(c) 100 Torr

Fig. 3. Particle-size distributions of the powders prepared at 40, 80, and 100 torr.

is truncated octahedral, which is in agreement with the observations of Teng *et al.*,¹⁰ who synthesized ultrafine alumina in a low-intensity, high-voltage arc.

The particle size increases slightly with increasing pressure. The particle size distributions of the powder prepared at 40, 80, and

Fig. 2. TEM micrographs of the nanostructured alumina powders prepared at chamber pressures of (a) 40 torr, (b) 80 torr, (c) 100 torr.

Table 1. Mean Particle Diameter (nm) and 95% Confidence Interval Assuming Lognormal Size Distributions

	40 Torr	80 Torr	100 Torr
Mean	21.3	24.1	24.1
95% CI	22.6 20.0	25.6 22.7	25.8 22.6

100 torr are shown in Fig. 3. They are approximately lognormal, with means and 95% confidence intervals (CI) of the means given in Table I. It can be seen that the mean particle diameter at 40 torr is a little less than that at 80 and 100 torr. It was not possible to carry the study to much lower pressures because the plasma became more diffuse and not all the aluminum was oxidized, resulting in metallic aluminum in the product.

Electron diffraction was used to examine the crystal structure of the powders. The results support the conclusions derived from the X-ray diffraction, i.e., there are two phases, γ and δ , with the γ major phase. No other alumina phases were found. It was discovered that the δ phase can coexist with the γ phase in the same

particle. Figure 4 shows such an example. The diffraction patterns were recorded from a single particle, and there are two sets of patterns in it. The strong spots forming a square lattice arise from the γ phase. The weak spots come from δ phase with the lattice parameters $a = a_\gamma$ ($a_\gamma = 0.79$ nm), $b = 2a_\gamma$, $c = 1.5a_\gamma$; a_γ is the lattice parameter of γ -Al₂O₃. Some δ spots are superimposed with the γ spots. The relationship between γ and δ phase is $[100]_\gamma // [100]_\delta, [010]_\gamma // [010]_\delta$, and $[001]_\gamma // [001]_\delta$.¹¹

IV. Conclusions

Nanostructured γ -alumina with a little δ -alumina has been synthesized by combustion of aluminum powder in an oxygen microwave plasma. The rapid quench prevents the formation of θ - and α -alumina in the final product. A lower reaction chamber pressure not only increases the content of γ -alumina, but also decreases the particle size. The particles are observed to be truncated octahedral with mean particle sizes of 21–24 nm. Small amounts of δ -alumina coexist with γ -alumina in single particles, which implies that the δ phase was formed by transformation of the γ -alumina.

References

- 1J. A. Wang, X. Bokhimi, A. Morales, O. Novaro, T. Lopez, and R. J. Gomez, "Aluminum Local Environment and Defects in the Crystalline Structure of Sol-Gel Alumina Catalyst," *J. Phys. B., At., Mol. Opt. Phys.* **103**, 299–303 (1999).
- 2C. Pecharroman, I. Sobrados, J. E. Iglesias, T. G. Carreno, and J. Sanz, "Thermal Evolution of Transitional Aluminas Followed by NMR and IR Spectroscopies," *J. Phys. B., At., Mol. Opt. Phys.* **103**, 6160–70 (1999).
- 3J. M. Mchale, A. Auroux, A. J. Perrotta, and A. Navrotsky, "Surface Energies and Thermodynamic Phase Stability in Nanocrystalline Aluminas," *Science*, **277**, 788–91 (1997).
- 4P. J. Eng, T. P. Trainor, G. E. Brown, G. A. Waychunas, M. Newville, S. R. Sutton, and M. L. Rivers, "Structure of the Hydrated Alpha-Al₂O₃ (001) Surface," *Science*, **288**, 1029–33 (2000).
- 5M. Wilson, M. Exner, Y. M. Huang, and M. W. Finnis, "Transferable Model for the Atomistic Simulation of Al₂O₃," *J. Phys. B., At., Mol. Opt. Phys.* **54**, 15683–89 (1996).
- 6B. C. Lippens and J. J. Steggerda, *Physical and Chemical Aspects of Adsorbent and Catalysts*; pp.171. Edited by B. G. Linsen. Academic Press, New York, 1970.
- 7C. L. Thomas, *Catalytic Process and Proven Catalysts*. Academic Press, New York, 1970.
- 8R. W. McCabe, R. K. Usmen, K. Ober, and H. S. Gandhi, "The Effect of Alumina Phase-Structure on the Dispersion of Rhodium/Alumina Catalysts," *J. Catal.*, **151**, 385–93 (1995).
- 9M. I. Boulos, P. Fauchais, and E. Pfender, *Thermal Plasmas: Fundamentals and Applications*, Vol.1; pp. 6–8. Plenum Press, New York, 1994.
- 10M. H. Teng, L. D. Marks, and D. L. Johnson, "Particles Produced by an Arc Discharge," *J. Mater. Res.*, **12**, 235–43 (1997).
- 11I. Levin and D. Brandon, "Metastable Alumina Polymorphs: Crystal Structures and Transition Sequences," *J. Am. Ceram. Soc.*, **81**, 1995–2012 (1998). □

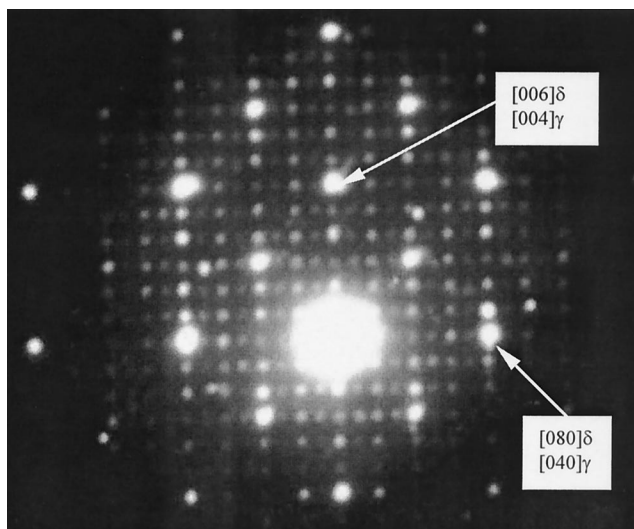


Fig. 4. Electron diffraction pattern of a nanostructured alumina particle containing both γ and δ phase; recorded along the $[100]$ axis.